A combined Sm–Nd, Rb–Sr, and U–Pb isotopic study of Mg-suite norite 78238: Further evidence for early differentiation of the Moon

J. Edmunson [a,*,1], L.E. Borg [b], L.E. Nyquist [c], Y. Asmerom [d]

[a] *Institute of Meteoritics, University of New Mexico, Albuquerque, NM 87131, USA*
[b] *Lawrence Livermore National Laboratory, Livermore, CA 94550, USA*
[c] *Johnson Space Center, Houston, TX 77058, USA*
[d] *Department of Earth and Planetary Sciences, University of New Mexico, Albuquerque, NM 87131, USA*

Abstract

Lunar Mg-suite norite 78238 was dated using the Sm–Nd, Rb–Sr, and U–Pb isotopic systems in order to constrain the age of lunar magma ocean solidification and the beginning of Mg-suite magmatism, as well as to provide a direct comparison between the three isotopic systems. The Sm–Nd isotopic system yields a crystallization age for 78238 of 4334 ± 37 Ma and an initial ε_{Nd}^{143} value of -0.27 ± 0.74. The age-initial ε_{Nd}^{143} (T-I) systematics of a variety of KREEP-rich samples, including 78238 and other Mg-suite rocks, KREEP basalts, and olivine cumulate NWA 773, suggest that lunar differentiation was completed by 4492 ± 61 Ma assuming a Chondritic Uniform Reservoir bulk composition for the Moon. The Rb–Sr isotopic systematics of 78238 were disturbed by post-crystallization processes. Nevertheless, selected data points yield two Rb–Sr isochrons. One is concordant with the Sm–Nd crystallization age, 4366 ± 53 Ma. The other is 4003 ± 95 Ma and is concordant with an Ar–Ar age for 78236. The ^{207}Pb–^{206}Pb age of 4333 ± 59 Ma is concordant with the Sm–Nd age. The U–Pb isotopic systematics of 78238 yield linear arrays equivalent to younger ages than the Pb–Pb system, and may reflect fractionation of U and Pb during sample handling. Despite the disturbed nature of the U–Pb systems, a time-averaged μ ($^{238}U/^{204}Pb$) value of the source can be estimated at 27 ± 30 from the Pb–Pb isotopic systematics. Because KREEP-rich samples are likely to be derived from source regions with the highest U/Pb ratios, the relatively low μ value calculated for the 78238 source suggests the bulk Moon does not have an exceedingly high μ value.
© 2008 Elsevier Ltd. All rights reserved.

1. INTRODUCTION

The lunar magma ocean (LMO) concept asserts that the mantle and crust of the Moon formed during solidification of a molten body by equilibrium and fractional crystallization (e.g., Smith et al., 1970; Wood et al., 1970; Snyder et al., 1992; Shearer and Papike, 1999). Lunar ferroan anorthosites (FANs) are thought to be floatation cumulates formed during the mid- to late-stage of LMO solidification. Following the formation of FANs, extreme fractionation during the last LMO stage concentrated incompatible elements into the KREEP (high K, rare earth element, and P) component, the signature of which is observed in the magnesium suite (Mg-suite), alkali suite, and KREEP basalts. Therefore, the LMO concept predicts that the FANs formed prior to KREEP, and both were followed by the Mg-suite. However, due to the overlapping crystallization ages determined for FANs and Mg-suite samples, as well as the model ages calculated for the formation age of KREEP, the age of LMO solidification is not precisely constrained by the present data set (Fig. 1).

* Corresponding author. Fax: +1 256 961 7215.
E-mail address: Jennifer.E.Edmunson@nasa.gov (J. Edmunson).
[1] Present address: Marshall Space Flight Center, National Space Science and Technology Center, Huntsville, AL 35805, USA.
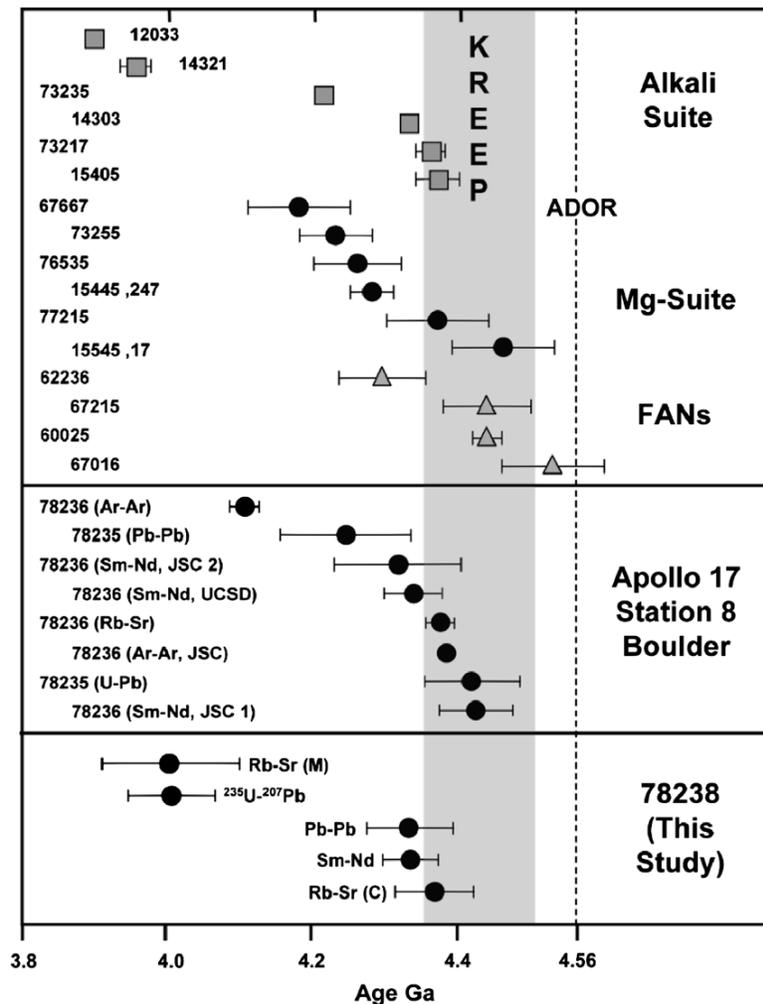
Fig. 1. Compilation of ages determined for old lunar rocks, the Apollo 17 Station 8 boulder, and 78238 (this study). Shaded area indicates the range of calculated KREEP model ages. Note the overlap between FANs, KREEP model ages, and the Mg-suite including previous ages for the Apollo 17 Station 8 boulder. Diagram modified from Borg et al. (1999) and references therein. Station 8 boulder citations are as follows: Ar–Ar, Aeschlimann et al. (1982); Pb–Pb, Hinthorne et al. (1977); Sm–Nd (UCSD), Carlson and Lugmair (1981); Rb–Sr, Ar–Ar, Sm–Nd 1 (JSC), Nyquist et al. (1981); U–Pb, Premo and Tatsumoto (1991); Sm–Nd 2 (JSC), Nyquist et al. (2008).

The apparent temporal overlap between FAN crystallization ages, KREEP model ages, and Mg-suite crystallization ages may stem from the inherent difficulties of dating these materials. For example, FANs are essentially monomineralic anorthosite, and contain only minor amounts of the mafic minerals required to determine a precise mineral isochron age for the sample. Additionally, the isotopic systematics of the FANs may have been disturbed during the post-crystallization impacts which formed the FAN breccias. Isotopic disturbances in FANs are suggested by their positive initial ε_{Nd}^{143} values (Carlson and Lugmair, 1988; Alibert, 1994; Alibert et al., 1994; Borg et al., 1999; Norman et al., 2003), which indicate derivation of FANs from a light rare earth element (LREE) depleted source relative to the Chondritic Uniform Reservoir (CHUR). This is inconsistent with the LMO model crystallization sequence from a Moon of bulk CHUR composition, which has mafic miner-

als crystallizing first and leaving a LREE-enriched melt from which the FANs formed. In this scenario, FANs should have initial ε_{Nd}^{143} values that are zero or slightly negative. It is also inconsistent with the calculated chondritic to LREE-enriched parent magma compositions for the FANs (e.g., Korotev et al., 1980). Therefore, if the measured Sm–Nd isotopic systematics of the FANs are not disturbed, they likely do not represent cumulates from a CHUR-like bulk Moon LMO and thus may not yield the correct age of LMO solidification.

It may be possible to date the minimum age of LMO solidification by dating the late-stage material that formed during LMO solidification, KREEP. Unfortunately, KREEP is only a component of some lunar rocks, and thus cannot be dated directly. Model ages for KREEP have been generated using the Sm–Nd and Rb–Sr isotopic systematics of KREEP-rich rocks and breccias, but are highly depen-

dent on the assumptions of the models. For example, an initial Sr isotopic composition for KREEP must be assumed for Rb–Sr model ages (e.g., Nyquist, 1977). It is also necessary to estimate the Rb abundance in KREEP using an average of assumed Sm/Rb ratios because of the volatile behavior of Rb and its potential loss during impact (Nyquist et al., 1972, 1973, 1974; Nyquist, 1977; Palme, 1977; Nyquist and Shih, 1992). Additionally, the ratio of parent to daughter elements in KREEP calculated using differentiation models are subject to uncertainties in the choice of partition coefficients, and this may inadvertently change the modeled age of KREEP formation. The shaded area of Fig. 1 shows that different assumptions made for different isotopic systems have yielded KREEP model ages that differ by almost 200 Ma (Lugmair and Carlson, 1978; Nyquist and Shih, 1992).

One emerging difficulty with the KREEP model ages, specifically those estimated from the ^{147}Sm–^{143}Nd isotopic system, is the assumption that KREEP is a product of the differentiation of a body with a CHUR bulk composition. This CHUR composition is assumed to be a well-defined, homogeneous starting composition for planetary bodies. However, recent papers (e.g., Boyet and Carlson, 2005; Rankenburg et al., 2006; Nyquist et al., 2008) indicate that specific CHUR values may need to be revised. For example, the howardite–eucrite–diogenite (HED) parent body has an initial ε_{Nd}^{143} value of +0.87 ± 0.25 (Nyquist et al., 2004) relative to CHUR, indicating that either the majority of samples originated in reservoirs with super-chondritic ^{147}Sm/^{144}Nd ratios, or the ^{143}Nd/^{144}Nd ratio of CHUR needs to be revised (Nyquist et al., 2008). A greater initial ^{143}Nd/^{144}Nd ratio than CHUR (ε_{Nd}^{143} of approximately +1) was determined for Precambrian terrestrial samples by Nägler and Kramers (1998), supporting the HED parent body initial ε_{Nd}^{143} value. In addition, Rankenburg et al. (2006) determined that lunar samples had chondritic ε_{Nd}^{142} values that are 20 parts per million less than terrestrial samples. Caro et al. (2008) claim that there is a difference in ^{142}Nd/^{144}Nd ratios between the Earth, Moon, Mars, and the asteroid belt, which is not due to imprecise measurements in previous studies, but is due to a higher ^{147}Sm/^{144}Nd ratio near the sun during accretion. If this is true, the positive initial ε_{Nd}^{143} values of some of the oldest FANs may be explained. However, the geochronology community has not yet adopted a new standard bulk composition for the Sm–Nd isotopic system. Some studies (e.g., Amelin and Rotenberg, 2004) still support the determined CHUR values. Therefore, the CHUR values of ^{143}Nd/^{144}Nd = 0.512638 and ^{147}Sm/^{144}Nd = 0.1967 will be employed for this study.

Further constraints, independent of bulk composition, can be placed on the minimum solidification age of the LMO by dating the oldest Mg-suite sample. The most reliable system commonly used to date the Mg-suite is ^{147}Sm–^{143}Nd because it seems to be the most resistant to disturbance associated with the late-heavy bombardment. The oldest ^{147}Sm–^{143}Nd age determined on a Mg-suite rock to date is 4460 ± 70 Ma (15445 ,17; Shih et al., 1993). However, this sample has a positive initial ε_{Nd}^{143} value, which does not agree with the derivation of the sample from a LREE-

enriched source relative to CHUR. The positive initial ε_{Nd}^{143} value determined for 15445 ,17 was the impetus for discussing a positive initial ε_{Nd}^{143} value of approximately +1 for the Moon by Shih et al. (1993). Alternatively, the age and initial ^{143}Nd/^{144}Nd ratio of this sample may indicate a misinterpreted bulk initial ^{143}Nd/^{144}Nd ratio for the Moon (e.g., $\varepsilon_{Nd}^{143} \sim +1$, Shih et al., 1993; $\varepsilon_{Nd}^{143} = +0.87$, Nyquist et al., 2006). If it is true that the bulk Moon has an initial ε_{Nd}^{143} that is positive, then 15445 ,17 may be the oldest Mg-suite sample dated. On the other hand, the age and initial of 15445 ,17 may indicate a LREE-depleted, previously differentiated reservoir parental to the KREEP-rich Mg-suite (e.g., Shih et al., 1993). Due to the multiple conclusions that may be drawn from the 15445 ,17 data, and the fact that this sample is often assumed to indicate the onset of Mg-suite magmatism, it is important to look at alternative samples that may further indicate the timing of KREEP formation or Mg-suite magmatism (e.g., 78238).

Magnesium-suite norite 78238 comes from the same Apollo 17 Station 8 boulder that has yielded some of the oldest ages for the Mg-suite rocks. The boulder is the parent to samples 78235, 78236, 78238, 78255, and 78256, and represents a single crystallization event (e.g., Jackson et al., 1975). Fig. 1 shows that ages previously obtained for samples from the Station 8 boulder using different isotopic systems range from 4110 ± 20 to 4430 ± 50 Ma (Nyquist et al., 1981; Aeschlimann et al., 1982). The multiple ages obtained for rocks from the Station 8 boulder indicate that the isotopic systematics are disturbed and likely reflect a variety of processes including igneous crystallization and impact metamorphism. There are two preferred ^{147}Sm–^{144}Nd ages and initial ε_{Nd}^{143} values obtained for 78236 by Carlson and Lugmair (1981) and Nyquist et al. (1981). The difference in the ages and initial ε_{Nd}^{143} values reported by the two groups stems from the interpreted isotopic resetting due to shock noted in the individual mineral fractions by Nyquist et al. (1981) and subsequently removed from the calculated isochron. Thus, the ages and initial ε_{Nd}^{143} values presented by Carlson and Lugmair (1981) and Nyquist et al. (1981) for 78236 are sufficiently different to warrant further study of the norites from the Station 8 boulder. The goal of this study is to define the age of this episode of Mg-suite norite formation using the Sm–Nd, Rb–Sr, and U–Pb isotopic systems and thereby constrain the age of LMO solidification and the beginning of Mg-suite magmatism. The same mineral fractions are used for all three systems to make each mineral fraction directly comparable in all three systems. In addition to determining the age of the norite, we hope to precisely determine the initial Nd, Sr, and Pb isotopic compositions of 78238 to better understand the primordial fractionation events associated with LMO solidification.

2. PETROLOGY OF THE STATION 8 BOULDER

The Apollo 17 Station 8 boulder was found at the base of the Sculptured Hills on the northwestern edge of the Serenitatis basin (Jackson et al., 1975). The boulder is approximately 0.5 m in diameter, has a subophitic cumulate texture, and is coated in glass. Samples from the boulder

are composed of approximately 50% chromian bronzite ($En_{78}Fs_{19}Wo_3$) and 50% plagioclase ($An_{93–97}$), with trace phases such as clinopyroxene, high-Si glass, K-feldspar, troilite, Fe-metal, oxides, and phosphates (e.g., Jackson et al., 1975; Sclar and Bauer, 1975; Table 1). Crystallization of the Station 8 boulder norites occurred with both ortho-pyroxene and plagioclase on the liquidus (Jackson et al., 1975). Jackson et al. (1975) postulated that the glass rind covering the boulder likely formed during ballistic transport. Winzer et al. (1975) noted that the composition of the glass rind matches the whole rock composition of the Station 8 boulder to a first order, which supports the formation of the rind during an excavation (shock metamorphism) event.

The minerals in the norite also show evidence of shock (e.g., Nyquist et al., 1981). Sclar and Bauer (1975) noted that the larger pyroxene grains have undulatory extinction, mosaicism, and planar deformation features. Carlson and Lugmair (1981) noted that the pyroxene grains were heavily fractured due to shock, which made the grains break apart easily during crushing as well as during magnetic separation and hand-picking procedures. Additionally, maskelynite (glassy plagioclase) formed from the plagioclase during a metamorphic event in which the boulder experienced shock pressures between 30 and 50 GPa and temperatures above 800 °C (Duke, 1968; Arndt and Gonzalez-Cabeza, 1981; Nyquist et al., 1981).

Compositional effects of shock have been observed in the pyroxene and plagioclase grains within the Apollo 17 Station 8 boulder impact melt (e.g., Sclar and Bauer, 1975). The pyroxenes in the impact melt veins of 78235 have a relatively high Al_2O_3 content (19–25%), and the plagioclase in the veins is relatively enriched in Fe and Mg when compared to the intact cumulate plagioclase (Sclar and Bauer, 1975). The increase in Fe and Mg in plagioclase within the veins is interpreted to be the incorporation of

small amounts of Fe metal and Mg-rich orthopyroxene into the plagioclase during shock (Sclar and Bauer, 1975; El Goresy et al., 1976; Mehta and Goldstein, 1980). Given the major element mobility that can occur in minerals during shock, it is possible that the minor elements, such as those of radiogenic isotopic systems, can be mobilized and redistributed during shock as well. These processes most likely account for the range in ages previously reported for samples from the Station 8 boulder.

3. ANALYTICAL METHODS

The chip of norite 78238 used in this study appeared to have an igneous texture, and did not show obvious signs of shock (e.g., shock melt veins) under visual inspection. However, the plagioclase was devitrified into maskelynite. Approximately 1.5 g of 78238 was crushed with a sapphire mortar and pestle. The grains were sieved in a stainless steel container through 100, 200, and 325-size nylon meshes. The 100–200 mesh fraction was then separated magnetically into six different mineral fractions (Fig. 2). The six mineral fractions were then hand-picked under a microscope at 94× magnification to the highest possible purity. Physical descriptions of the mineral fractions analyzed appear in Table 2. The hand-picked fractions were leached with 0.5 N acetic acid, rinsed with 4× quartz distilled water, and then sonicated with 2 N HCl at 25 °C for 10 min. The HCl (leachate) was removed from the residue fractions and not analyzed. Digestion of the residues was completed with small amounts of ultra-pure concentrated HF and HNO_3, and 6 N HCl acids. The mineral fractions were spiked with mixed $^{149}Sm–^{150}Nd$, $^{87}Rb–^{84}Sr$, and $^{233}U–^{236}U–^{205}Pb$ tracer solutions. The initial chemical separation (U and Pb from Rb + Sr + REE) was completed at the Radiogenic Isotope Laboratory at the University of New Mexico (UNM), using Eichrom analytical grade anion exchange resin 1×8, 200–400 mesh, in 50, 100, and 250 μL columns and eluting in 4× quartz distilled HCl, HNO_3, and HBr. The Rb + Sr + REE cut was transferred to the Radiogenic Isotope Laboratory at the Johnson Space Center (JSC) for the final chemical separation. The JSC chemical procedures involved separation of Rb, Sr, and REE using 2 and 6 N HCl, and AG50x8 cation resin. Separation of individual REEs was completed with alpha-hydroxyisobutyric acid (α-HIBA) and NH_4-form AG50x8 resin. The Rb and Sr isotope analyses were completed with a Finnigan MAT 261 thermal ionization mass spectrometer (TIMS) at JSC. The U, Pb, Sm, and Nd isotopic ratios were determined at UNM using a VG Sector 54 TIMS. Neodymium isotopic measurements were normalized to $^{146}Nd/^{144}Nd = 0.7219$. Neutron fluence effects were measured by analyzing a separate whole rock sample for the Sm isotopic composition. The following blank corrections were incorporated into the data reduction calculations: Rb = 10 pg, Sr = 40 pg, Sm = 20 pg, Nd = 20 pg, and U = 3 pg. The Pb blank corrections varied for each sample, from 12 to 70 pg, and were dependent on the amount of mixed $^{87}Rb–^{84}Sr$ tracer solution added. Because of the low abundance of ^{204}Pb in lunar materials, Pb analyses were conducted by measuring ^{204}Pb in a Daly

Table 1
Modal mineralogy of thin sections from the Apollo 17 Station 8 boulder.

Samples	78235,6[a]	78235,49[b]	78236,8[c]	78238[a,d]
Orthopyroxene	51	51.2	53.6	32
Clinopyroxene	0.01	0.01	0.6	<0.1
Plagioclase	48	48.2	39.2	68
High-Si glass	0.25	0.25	2.4	Trace
K-feldspar	Trace		Trace	Trace
Phosphate	0.03	0.032	Trace	Trace
Baddeleyite	Trace	Trace		Trace
Zircon	Trace	Trace		Trace
Troilite	Trace	Trace	Trace	
Ilmenorutile	Trace	Trace	Trace	Trace
Ilmenite				Trace
Chromite	Trace	Trace	Trace	Trace
Fe metal	Trace	Trace	Trace	
Impact melt			4.0	

[a] James and Flohr (1983).
[b] McCallum and Mathez (1975).
[c] Nyquist et al. (1981).
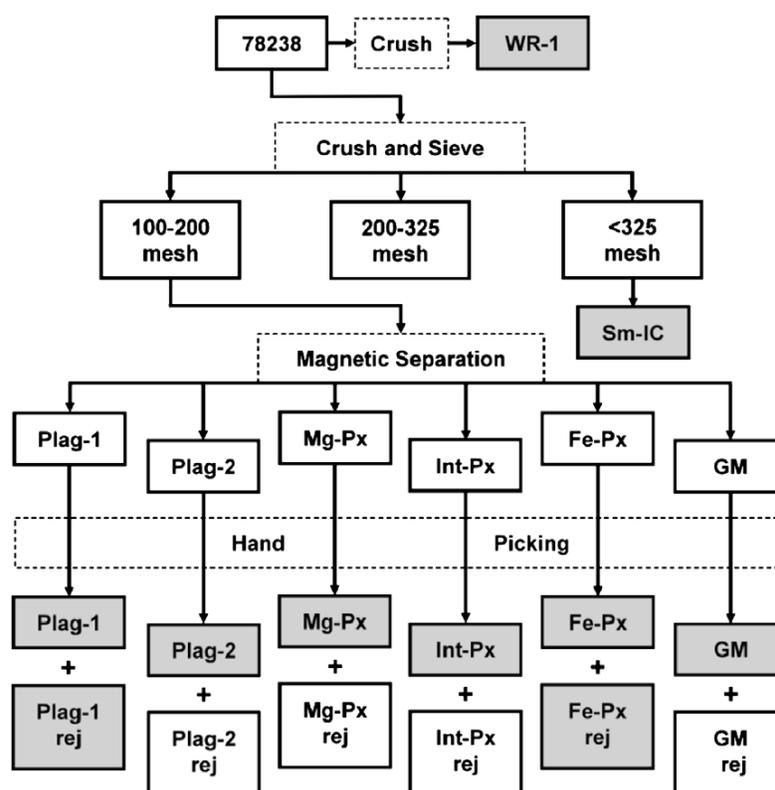[d] Unspecified thin section(s).

Fig. 2. Flow diagram illustrating the mineral separation procedure. Processes and products are outlined in dashed and solid lines, respectively. Gray blocks indicate fractions that were analyzed during this study. See text for detail.

Table 2
Descriptions of analyzed mineral fractions.

Mineral fraction	Purity (%)	Description
Plag-1	>99.9	Glassy plagioclase with conchoidal fracture. No visible impurities.
Plag-1 rej	95–97	Glassy plagioclase. Some grains appear milky white (devitrified?). Flow banding of impurities within grains. Possible impurities include impact melt and phosphates.
Plag-2	97	Glassy plagioclase. Impact melt and vesicles appear as small bubbles inside the glass.
Mg-Px	90	Light green to yellowish, sometimes translucent pyroxene. Small oxides and impact melt appear on grain boundaries. Dominant impurities include impact melt and glassy plagioclase.
Int-Px	>99	Light green, opaque pyroxene. Some grains have a darker green hue.
Fe-Px	>99.9	Very light green, opaque pyroxene. No visible impurities.
Fe-Px rej	90	Light to dark green pyroxene. 90% of pyroxene was opaque, the other 10% was translucent. Impurities in this fraction include ∼5% glassy plagioclase and ∼5% impact melt.
GM	25	Composed of ∼65% pyroxene, ∼25% impact melt and oxides, and ∼10% glassy plagioclase. This glass and mesostasis (interstitial material)-rich fraction was meant to have a high impurity content, and represent the "reject" component of the other mineral fractions.

All fractions picked at 94× magnification.

multiplier and [205]Pb (tracer), [206]Pb, [207]Pb, and [208]Pb on Faraday collectors. The relative gain between the Daly and Faraday collectors was measured and corrected for in each analysis. Isochrons were calculated with Isoplot 2.49 (Ludwig, 2001) with 2σ errors. The points chosen for use in the isochron calculations are the maximum number for a reasonable linear array. Values for isotopic standards are given in the data tables.

4. RESULTS AND DISCUSSION

4.1. Sm–Nd isotopes

The [147]Sm–[143]Nd isochron obtained for 78238 indicates a crystallization age of 4334 ± 37 Ma with an initial ε_{Nd}^{143} value of −0.27 ± 0.74 (Fig. 3 and Table 3). Despite the presence of impurities such as impact melt in many fractions
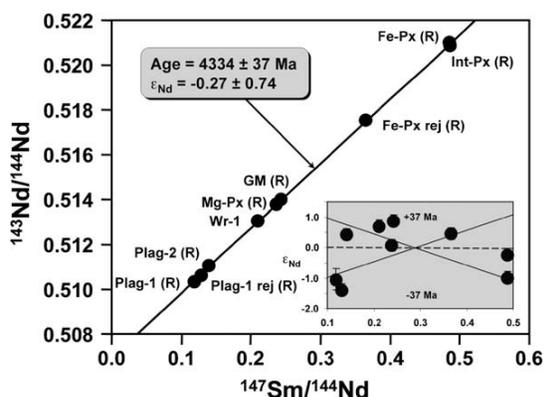
Fig. 3. ^{147}Sm–^{143}Nd isochron for 78238. Age of 4334 ± 37 Ma and initial ε_{Nd}^{143} value of −0.27 ± 0.74 determined from all nine data points. Wr = whole rock, Plag = plagioclase, Px = pyroxene, Int = intermediate magnetic separation, GM = glass and mesostasis (interstitial material)-rich fraction, rej = portion rejected during hand-picking, (R) indicates residue after acetic and HCl leaches. Isochron mean standard weighted deviation (MSWD) is 13. Initial ε_{Nd}^{143} calculated using the method of Fletcher and Rosman (1982). Inset indicates deviation of each point from the isochron in ε_{Nd}^{143} notation $(\varepsilon_{Nd}^{143} = [(^{143}Nd/^{144}Nd)^{measured}/(^{143}Nd/^{144}Nd)^{isochron} - 1] \times 10^4)$.

(Table 2), the isochron is defined by all nine fractions. The non-ideal MSWD of 13 may indicate a slight disturbance of the Sm–Nd isotopic systematics in the individual mineral fractions, but it is insufficient to alter the determined age of the sample or the initial outside the calculated error. The Sm–Nd age of 78238 is younger than the 4460 ± 70 Ma age obtained on clast 17 of Mg-suite rock 15445 (Shih et al., 1993) and is younger than the age preferred for 78236 by Nyquist et al. (1981), but it is concordant with the ages of 78236 by Carlson and Lugmair

(1981), 78235/78236 (mixed) by Premo (1991), and a revised age for 78236 by Nyquist et al. (2008).

The near-CHUR to slightly negative initial ε_{Nd}^{143} value of 78238 is important because it is more consistent with petrogenetic models for the production of Mg-suite rocks from LREE-enriched parent magmas relative to CHUR. Indeed, parental melt compositions calculated from Mg-suite norites show the dominance of the KREEP component in the REE signatures of the parental melts (e.g., Papike et al., 1996). If the KREEP component in the Mg-suite was the result of the initial differentiation of a Moon with a bulk composition equal to CHUR (present-day ^{147}Sm/^{144}Nd = 0.1967, ^{143}Nd/^{144}Nd = 0.512638, $\varepsilon_{Nd}^{143} \equiv 0$), then all Mg-suite samples should have chondritic to slightly negative initial ε_{Nd}^{143} values.

Fig. 4 illustrates the relationship between crystallization ages and initial ε_{Nd}^{143} values for lunar materials containing a KREEP signature. The samples that lie below the chondritic evolution line define a single evolution line, within analytical uncertainty, anchored on one end by the KREEP-rich olivine cumulate clast in NWA 773 and on the other by 78238. This evolution line implies that the Mg-suite samples with negative initial ε_{Nd}^{143} values, as well as the KREEP basalts, were derived from a source or sources with a ^{147}Sm/^{144}Nd ratio of 0.178 ± 0.006. It is significant that this ^{147}Sm/^{144}Nd ratio is shared by all lunar samples that have negative ε_{Nd}^{143} values because it suggests that the KREEP component incorporated into the Mg-suite and KREEP basalts had a common source, or the KREEP components were derived by a similar extent of fractional crystallization of the bulk Moon. Note however that the presence of a KREEP component in both the Mg-suite and KREEP basalt source region will dominate the REE signature in both suites of rocks. Thus, the fact that all KREEP-rich samples appear to be derived from sources with common ^{147}Sm/^{144}Nd ratios does not imply that their sources are identical.

Table 3
Sm–Nd analytical results for 78238.

Fraction	Wt (mg)	Sm (ppm)	Nd (ppm)	$\frac{^{147}Sm^a}{^{144}Nd}$	$\frac{^{143}Nd^b}{^{144}Nd}$
Wr 1	12.02	1.419	4.071	0.21074 ± 21	0.513071 ± 20
Plag-1 (R)	2.98	0.856	4.350	0.11902 ± 48	0.510346 ± 36
Plag-1 rej (R)	8.09	0.980	4.563	0.12987 ± 17	0.510639 ± 20
Plag-2 (R)	2.81	0.732	3.136	0.14104 ± 70	0.511053 ± 20
Mg-Px (R)	15.82	0.936	2.380	0.23782 ± 24	0.513815 ± 20
Int-Px (R)	21.82	0.603	0.749	0.48644 ± 49	0.520945 ± 20
Fe-Px (R)	17.17	0.610	0.759	0.48537 ± 63	0.520887 ± 22
Fe-Px rej (R)	58.78	0.658	1.088	0.36567 ± 37	0.517503 ± 20
GM (R)	9.81	1.023	2.553	0.24216 ± 26	0.513975 ± 20
LaJolla Nd (N = 3)					0.511893 ± 19[c]

Chemical separations performed at JSC, mass spectrometry performed at UNM. All samples and standards run as NdO$^+$. Sm concentration calculated using natural ^{147}Sm/^{152}Sm = 0.560828 (norm), ^{149}Sm/^{152}Sm = 0.515490 ± 2, and ^{150}Sm/^{152}Sm = 0.277439 ± 5 to correct for neutron fluence, $\varepsilon_{Sm} = 0.00271 ± 3$.
Isochron are calculated using either $2\sigma_p$ (from standard runs) or $2\sigma_m$ (from measured isotopic ratios), whichever is larger.
[a] Error limits apply to last digits and include a minimum uncertainty of 0.5% plus 50% of the blank correction for Sm and Nd added quadratically.
[b] Normalized to ^{146}Nd/^{144}Nd = 0.7219. Uncertainties refer to last digits and are $2\sigma_m$ calculated from the measured isotopic ratios. $2\sigma_m = [\Sigma(m_i - \mu)^2/(n(n-1))]^{1/2}$ for n ratio measurements m_i with mean value μ.
[c] Error limits refer to last digits and are $2\sigma_p$. $2\sigma_p = [\Sigma(M_i - \pi)^2/(N-1)]^{1/2}$ for N measurements M_i with mean value π.
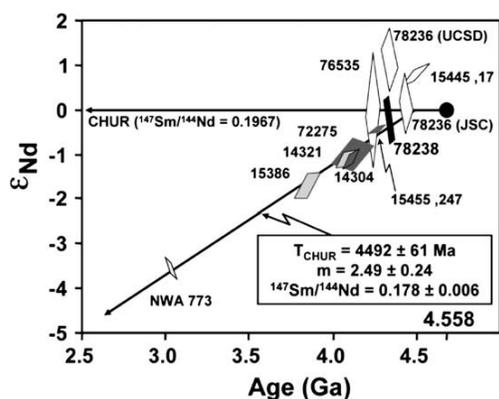
Fig. 4. Time vs. initial ε_{Nd}^{143} value diagram, illustrating the relationship between the Mg-suite and KREEP rocks (14304, Snyder et al., 1995; 14321, Shih et al., 1985; 15386, Carlson and Lugmair, 1979; 15445 ,17 and 15455 ,247, Shih et al., 1993; 72275, Shih et al., 1992; 76535, Lugmair et al., 1976; 78236 JSC, Nyquist et al., 1981; 78236 UCSD, Carlson and Lugmair, 1981; NWA 773, revised from Borg et al., 2004; 78238, this study). Black circle = chondritic starting composition at 4558 Ma, black polygon = 78238, white polygons = Mg-suite samples with positive ε_{Nd}^{143} values, dark gray polygons = Mg-suite samples with negative ε_{Nd}^{143} values, light gray polygons = KREEP basalts and olivine cumulate NWA 773. The line regressed through the KREEP-rich samples with negative ε_{Nd}^{143} values indicates a common fractionation history for the KREEP signature of these rocks from a source region with a $^{147}Sm/^{144}Nd$ ratio of 0.178 ± 0.006. All samples in this diagram have been renormalized to a La Jolla Nd standard value of 0.511850. The revised age and initial ε_{Nd}^{143} of NWA 773 is 3032 ± 32 Ma and −3.51 ± 0.27, respectively (Borg et al., 2005b). New data from Nyquist et al. (2008) for 78236 overlaps the 78238 data and is not represented in the figure.

A model age for KREEP formation, and hence the minimum age for the completion of silicate differentiation, is defined by the intersection of the $^{147}Sm/^{144}Nd = 0.178$ evolution line with the CHUR evolution line in Fig. 4. The resulting model age is 4492 ± 61 Ma, which is consistent with the $^{176}Lu–^{176}Hf$ data obtained by Taylor et al. (2007) and U–Pb estimates of lunar KREEP reservoir formation (e.g., >4370 Ma; Nemchin et al., 2008) from lunar zircons. The $^{147}Sm–^{143}Nd$ model age for KREEP is also within uncertainty of the Rb–Sr estimate of 4420 ± 70 Ma for KREEP formation by Nyquist and Shih (1992), which assumes an initial Sm/Rb ratio for KREEP of 2.3. However, the $^{147}Sm–^{143}Nd$ age is not within uncertainty of the estimates of lunar silicate differentiation by the $^{146}Sm–^{142}Nd$ isotopic system of 4320^{+56}_{-40} Ma (Nyquist et al., 1995) or 4343^{+23}_{-21} (Rankenburg et al., 2006). This implies that the $^{146}Sm–^{142}Nd$ system does not record the age of LMO solidification, but rather is disturbed by events occurring after the Moon solidified (e.g., Borg and Wadhwa, 2006).

It is important to address the Mg-suite samples with positive ε_{Nd}^{143} values. As mentioned above, it may be possible that the bulk composition of the Moon has a slightly positive ε_{Nd}^{143} value compared to the CHUR value. If this is true, and the relationship between the younger KREEP-rich

rocks and the Mg-suite is firm, samples 76535 and norite 78236 (JSC; Nyquist et al., 1981) would also lie along the KREEP trend. Incorporating these samples into the linear regression and using a value greater than $\varepsilon_{Nd}^{143} = 0$ for the bulk Moon would only *increase* the age of primary lunar differentiation. Thus, this is a strong argument against relatively young primary differentiation ages for the Moon.

The $^{147}Sm–^{143}Nd$ isotopic systematics of KREEP-rich samples share several characteristics with rocks derived from LREE-enriched sources on Mars. For example, the lunar KREEP model age of 4492 ± 61 Ma is concordant with the ε_{Nd}^{142} - ε_{Nd}^{143} model age of 4526^{+21}_{-19} Ma suggested for martian differentiation (Borg et al., 1997, 2005a; Borg and Drake, 2005; Foley et al., 2005). Additionally, similar $^{147}Sm/^{144}Nd$ ratios calculated for lunar KREEP (0.178) and "martian KREEP" (0.182; Borg and Draper, 2003) suggest similar processes may be involved in producing each of these evolved, incompatible element-rich components. If the evolved component in both the Moon and Mars represents a late-stage liquid derived by crystallization of a magma ocean, the similar $^{147}Sm/^{144}Nd$ ratios of the evolved source regions may indicate both lunar and martian magma oceans had similar evolutionary histories.

4.2. Rb–Sr isotopes

The Rb–Sr data for 78238 are disturbed. Nevertheless, two isochrons with apparent age significance can be derived by choosing specific data points (Fig. 5 and Table 4). The oldest age of 4366 ± 53 Ma is defined by the Plag-2, whole rock, and Mg-Px fractions. This age is concordant with the Sm–Nd age of 78238, and is also interpreted to represent the crystallization age (C) of the sample. The remaining fractions, as well as the whole rock, define a younger age (M) of 4003 ± 95 Ma. This age is interpreted to represent the time at which the Rb–Sr isotopic systematics of 78238 were disturbed by metamorphism. This conclusion is based on the fact that the youngest Rb–Sr age (M) is concordant with an Ar–Ar age of 4110 ± 20 Ma obtained for a plagioclase separate from 78236 by Aeschlimann et al. (1982). Since both of the Rb–Sr isochrons presented in Fig. 5 contain the whole rock, the disturbance observed in the Rb–Sr isotopic systematics appears to be a rotation of the isochron about the whole rock (e.g., Nyquist et al., 1981, 1991a,b).

Isochron rotation is a likely result of the isotopic re-equilibration of minerals within a rock, without the loss (or gain) of either the parent or daughter element from the system. A mechanism that could explain the rotation of an isochron about the whole rock is post-crystallization isotopic re-homogenization via a metamorphic event. The observation that the Plag-2 and Mg-Px fractions define the crystallization age of Fig. 5 suggests that these fractions behave differently during metamorphism than the other mineral fractions. One possible difference between the fractions that lie on the two isochrons which could account for their incongruous responses to metamorphism is the quantity of interstitial material in the fractions. During a shock event, interstitial material can isotopically re-equilibrate within a relatively short amount of time (e.g., Carlson and Lugmair, 1981). This is presumably a result of the
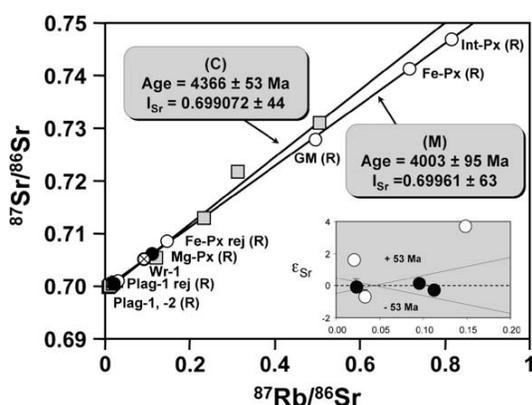
Fig. 5. Rb–Sr isochron diagram for 78238 (circles) and 78236 (squares, Nyquist et al., 1981). The oldest ^{87}Rb–^{86}Sr isochron, drawn through the Plag-2, Wr-1, and Mg-Px fractions (black circles), yields an age of 4366 ± 53 Ma with an initial ^{87}Sr/^{86}Sr of 0.699072 ± 44 and a MSWD of 0.27. This age is concordant with the Sm–Nd age obtained for 78238 in this study (4322 ± 40 Ma), as well as a 78236–78238 whole rock Rb–Sr isochron age (4343 ± 48 Ma). It is interpreted to represent the crystallization age of the sample, and is referred to as (C). The remaining fractions (white dots), as well as the Wr-1, define an age of 4003 ± 95 Ma, with an initial ^{87}Sr/^{86}Sr of 0.69961 ± 63 Ma and a MSWD of 65. This young Rb–Sr age is concordant with an Ar–Ar age for 78236 of 4110 ± 20 Ma (Aeschlimann et al., 1982) as well as the ^{235}U–^{207}Pb age obtained in this study, and likely represents the age of metamorphism of 78238 (M). Inset indicates the deviation of the points used to define the (C) isochron age in ε_{Sr} notation. The ^{87}Rb decay constant used in the age calculation is 1.402×10^{-11} y^{-1} (Minster et al., 1982).

inability of glass to restrict elemental diffusion. The Plag-2 and Mg-Px mineral fractions may have relatively low abundances of interstitial material and are consequently more resistant to re-equilibration than the fractions with high abundances of interstitial material. Therefore, an isochron containing the Plag-2 and Mg-Px fractions, as well as the whole rock, could be more likely to reflect the age of crystallization of 78238. Those fractions containing an appreciable amount of interstitial material will isotopically re-equilibrate more readily than the Plag-2 and Mg-Px fractions, resulting in rotation of an isochron defined by the interstitial material-rich fractions. In this scenario, the 4003 ± 95 Ma isochron represents the age of the metamorphic event.

Resetting of the Rb–Sr system in interstitial material-rich fractions of 78238 is supported by a two-point whole rock Rb–Sr "isochron" for the Apollo 17 Station 8 boulder. This isochron is defined by the whole rock analyses from 78236 from Nyquist et al. (1981) and 78238. A whole rock isochron can be used for this boulder because the modal mineralogy of the 78236 and 78238 whole rocks analyzed differ enough to provide a spread in ^{87}Rb/^{86}Sr and ^{87}Sr/^{86}Sr ratios. The crystallization age of the Station 8 boulder determined by this method is 4343 ± 48 Ma, which is concordant with the 4334 ± 37 Ma Sm–Nd isochron age presented above. The fact that the whole rock crystallization age for the Station 8 boulder norites is concordant with the Sm–Nd internal isochron age of 78238 indicates that the Rb–Sr isotopic systematics of the boulder have remained closed during the disturbance that appears to have re-homogenized the Rb–Sr system between various igneous phases.

The initial ^{87}Sr/^{86}Sr isotopic composition for 78238 from the (C) isochron ($T = 4366 \pm 53$ Ma) is 0.699072 ± 0.000044, which is slightly higher than that of Angra dos Reis (ADOR, 0.698970 ± 0.000018; Nyquist et al., 1994) and the Basaltic Achondrite Best Initial (BABI, 0.69898 ± 0.00003; Papanastassiou and Wasserburg, 1969), and is within uncertainty of LUNI (0.69903, Nyquist et al., 1973), indicating relatively little production of ^{87}Sr in the source region of 78238. The initial ^{87}Sr/^{86}Sr for 78238

Table 4
Rb–Sr analytical results for 78238.

Fraction	Wt (mg)	Rb (ppm)	Sr (ppm)	$\frac{^{87}Rb^a}{^{86}Sr}$	$\frac{^{87}Sr^b}{^{86}Sr}$
Wr 1	12.02	1.00	30.97	0.09426 ± 47	0.705041 ± 10
Plag-1 (R)	2.98	1.36	199.3	0.01974 ± 10	0.700434 ± 10
Plag-1 rej (R)	8.09	2.16	193.2	0.03227 ± 16	0.701065 ± 13
Plag-2 (R)	2.81	1.51	193.6	0.02250 ± 11	0.700492 ± 15
Mg-Px (R)	15.82	1.22	31.71	0.11139 ± 56	0.706089 ± 11
Int-Px (R)	21.82	0.082	0.290	0.8131 ± 41	0.746736 ± 27
Fe-Px (R)	17.17	0.063	0.256	0.7164 ± 46	0.741230 ± 31
Fe-Px rej (R)	58.78	0.453	8.91	0.14701 ± 74	0.708622 ± 10
GM (R)	9.81	3.12	18.23	0.49573 ± 48	0.727904 ± 12
NBS-987 ($N = 6$)					0.710247 ± 10^c

Chemical separations and mass spectrometry performed at JSC. ^{85}Rb/^{87}Rb ratio of two runs of the NBS-727 Rb standard = 2.5976 ± 31 ($2\sigma_p$). λ^{87}Rb = 1.402×10^{-11} y^{-1}.
Isochrons are calculated using either $2\sigma_p$ (from standard runs) or $2\sigma_m$ (from measured isotopic ratios), whichever is larger.
[a] Error limits apply to last digits and include a minimum uncertainty of 0.5% plus 50% of the blank correction for Rb and Sr added quadratically.
[b] Normalized to ^{86}Sr/^{88}Sr = 0.1194. Uncertainties refer to last digits and are $2\sigma_m$ calculated from the measured isotopic ratios. $2\sigma_m = [\Sigma(m_i - \mu)^2/(n(n-1))]^{1/2}$ for n ratio measurements m_i with mean value μ.
[c] Uncertainties refer to last digits and are $2\sigma_p$. $2\sigma_p = [\Sigma(M_i - \pi)^2/(N-1)]^{1/2}$ for N measurements M_i with mean value π.

(and 78236, 0.69907 ± 0.00002; Nyquist et al., 1981) is within error of previously studied Mg-suite samples (e.g., 72417, 0.69900 ± 0.00004, Papanastassiou and Wasserburg, 1975; 76535, 0.69900 ± 0.00003, Papanastassiou and Wasserburg, 1976; 77215, 0.69901 ± 0.00007, Nakamura et al., 1976; 15455, 0.69899 ± 0.00006, Shih et al., 1993). The two-point whole rock isochron from the Station 8 boulder is also in agreement and has an initial of 0.699044 ± 0.000055. The fact that the initial Sr isotopic composition of the Mg-suite is so similar to ADOR, BABI, and LUNI indicates that the $^{87}Rb/^{86}Sr$ ratios of the sources are low and the source regions formed fairly close to the formation age of the Solar System. Estimates of the source region $^{87}Rb/^{86}Sr$ ratio for the Mg-suite, assuming a single-stage evolution from both ADOR and BABI, yield a range of 0.01 to 0.06 (Nakamura et al., 1976; Nyquist et al., 1981; Shih et al., 1993), with 78238 at 0.03 ± 0.01.

4.3. U–Pb isotopes

The Pb–Pb age obtained for 78238 is 4333 ± 59 Ma and is concordant with the Sm–Nd and Rb–Sr (C) ages (Fig. 6 and Table 5). The mineral fractions dominated by plagioclase (maskelynite) were not used in the calculation of the Pb–Pb isochron. These plagioclase-dominated fractions, which show the greatest physical change due to shock when compared to the other mineral fractions (Table 2), have higher $^{207}Pb/^{204}Pb$ ratios for given $^{206}Pb/^{204}Pb$ ratios than the remaining mineral fractions and whole rock (i.e., they lie above the Pb–Pb isochron). The relatively elevated $^{207}Pb/^{204}Pb$ ratios of the plagioclase fractions may reflect the incorporation of a component with an enriched $^{207}Pb/^{206}Pb$ ratio. The enriched $^{207}Pb/^{206}Pb$ component is likely from an old, differentiated source characterized by a high μ ($^{238}U/^{204}Pb$) value, such as lunar soil (Unruh and Tatsumoto, 1977; Hanan and Tilton, 1987; Premo and Tatsumoto, 1991; Premo et al., 1999). This component

Fig. 6. Pb–Pb isochron for 78238 defining an age of 4333 ± 59 Ma. This age is concordant with the Sm–Nd age and the Rb–Sr (C) age obtained for 78238 during this study. Note that the plagioclase fractions fall off the isochron in the direction of lunar soil compositions (shaded) of Premo et al. (1999). The MSWD of the isochron is 15,948. Nevertheless, the large spread in the data results in a line with the appropriate slope.

could be added to the plagioclase during melting and flow associated with thermal metamorphism.

The deviation of the plagioclase fractions from the 78238 Pb–Pb isochron, as well as the tendency of the plagioclase fractions to have anomalously high $^{207}Pb/^{206}Pb$ ratios, is emphasized in Fig. 7a (after Tera and Wasserburg, 1972; Premo et al., 1999). Incorporation of a component with a high $^{207}Pb/^{206}Pb$ ratio, such as lunar soil Pb, could occur during the shock event(s) that melted the plagioclase in 78238 (e.g., Misawa et al., 2000). However, Papike et al. (1982) noted that the soil at the Apollo 17 Station 8 site had high Sm and Nd abundances, which could also influence the linearity of the 78238 Sm–Nd isochron if the soil were only incorporated into the plagioclase fractions in large quantity. Because the 78238 Sm–Nd isochron does not show evidence for soil addition into the plagioclase fractions it is likely that insufficient soil was added to influence the Sm–Nd isotopic composition of the plagioclase fractions (e.g., the Nd/Pb of the soil is too low), the soil added had a nearly identical Sm–Nd isotopic signature as the plagioclase fractions of 78238, or the high $^{207}Pb/^{206}Pb$ component added was elemental Pb mobilized by impact volatility (e.g., Misawa et al., 2000). There is no apparent disturbance to the Pb isotopic systematics of the mafic silicate and whole rock fractions. Accordingly, the line running through the mafic silicate and whole rock fractions in Fig. 7a intersects the ordinate at a $^{207}Pb/^{206}Pb$ ratio indicative of an age of 4288 ± 27 Ma, which is concordant with the Sm–Nd crystallization age determined for 78238.

Unfortunately, the $^{235}U-^{207}Pb$ and $^{238}U-^{206}Pb$ linear arrays obtained for 78238 (not shown) are not concordant with the Sm–Nd, Rb–Sr (C), or the Pb–Pb age. The $^{235}U-^{207}Pb$ linear array corresponds to an age for 78238 of 4010 ± 60 Ma and is concordant with the disturbed Rb–Sr (M) age of 4003 ± 95 Ma. The $^{238}U-^{206}Pb$ linear array corresponds to an age of 3520 ± 290 Ma and is not concordant with any age determined for this rock. Discordant U–Pb "ages", specifically those where the $^{238}U-^{206}Pb$ age is younger than the $^{235}U-^{207}Pb$ age have been reported for lunar troctolite 76535 (Premo and Tatsumoto, 1992), as well as mare basalts 10017 (Gaffney et al., 2007) and 15085 (Unruh and Tatsumoto, 1977). The contribution of terrestrial Pb (chemistry blank) to the fractions may contribute to the discordance between the Pb–Pb and both U–Pb ages due to the large difference between lunar and terrestrial Pb isotopic compositions. However, increasing the blank contribution to the U–Pb isotopic systems will decrease both U–Pb ages equally, resulting in young but concordant $^{235}U-^{207}Pb$ and $^{238}U-^{206}Pb$ ages. In addition, the leaching procedure followed in this study is identical to that of Gaffney et al. (2007), which shows that all possible surficial terrestrial Pb, as well as some lunar Pb, is removed by this leaching procedure. Therefore, terrestrial contamination is probably not responsible for the separation in $^{235}U-^{207}Pb$ and $^{238}U-^{206}Pb$ ages observed in 78238. Note that the estimated isotopic composition of terrestrial Pb (Stacey and Kramers, 1975) lies within uncertainty of the 78238 Pb–Pb isochron (Fig. 6). Therefore, mixing the mineral fractions with terrestrial Pb would only draw the points down the Pb–Pb isochron toward the origin. In fact, increasing
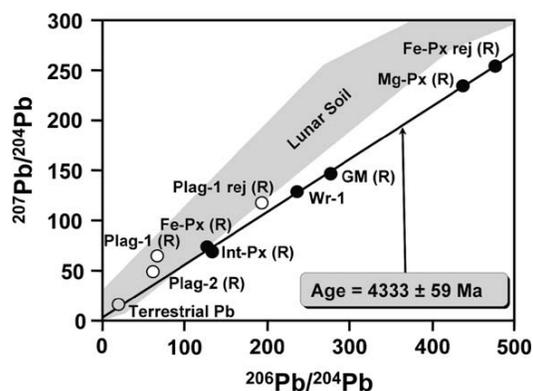
Table 5
U–Pb analytical results for 78238.

Fraction	Wt (mg) ID, IC	Pb (ppm)	U (ppm)	$\frac{204\text{Pb}}{206\text{Pb}}$[a]	$\frac{207\text{Pb}}{206\text{Pb}}$[a]	$\frac{238\text{U}}{204\text{Pb}}$[b]	Pb blank (pg)
Wr 1	12.02, —	0.169	0.104	0.004271 ± 2	0.53531 ± 3	275.804 ± 4.768	69
Plag-1 (R)	2.98, —	0.042	0.021	0.015444 ± 10	1.03504 ± 31	85.307 ± 14.425	38
Plag-1 rej (R)	8.09, —	0.183	0.195	0.005205 ± 2	0.60272 ± 4	404.704 ± 7.736	56
Plag-2 (R)	2.81, 22.48	0.081	0.037	0.016830 ± 25	0.82417 ± 68	76.637 ± 6.585	38
Mg-Px (R)	1.96, 13.86	0.204	0.131	0.002299 ± 3	0.53769 ± 12	579.299 ± 18.762	24
Int-Px (R)	2.67, 19.15	0.035	0.024	0.007600 ± 19	0.57592 ± 85	187.764 ± 18.418	16
Fe-Px (R)	2.11, 15.06	0.036	0.019	0.007956 ± 8	0.57396 ± 16	145.062 ± 17.119	14
Fe-Px rej (R)	7.21, 51.31	0.085	0.061	0.002110 ± 2	0.53599 ± 9	641.411 ± 29.013	53
GM (R)	1.18, 8.62	1.120	0.783	0.003648 ± 3	0.53684 ± 10	337.830 ± 4.712	33
NBS-981 ($N = 6$)					0.059207 ± 42[c]		12

Chemical separations and mass spectrometry performed at UNM. Pb ID used for concentration, Pb IC used for Pb isotopic ratios. Pb blank listed is the highest calculated blank for each fraction.

Isochrons are calculated using either $2\sigma_p$ (from standard runs) or $2\sigma_m$ (from measured isotopic ratios), whichever is larger.

[a] Uncertainties are $2\sigma_m$ calculated from the measured isotopic ratios. $2\sigma_m = [\Sigma(m_i - \mu)^2/(n(n-1))]^{1/2}$ for n ratio measurements m_i with mean value μ. Error reported applies to the last significant figure in the ratio.

[b] Error limits include a minimum uncertainty of 0.5% plus 50% of the blank correction for U and Pb added quadratically. Error stated is absolute error.

[c] Uncertainties are $2\sigma_p$. $2\sigma_p = [\Sigma(M_i - \pi)^2/(N-1)]^{1/2}$ for N measurements M_i with mean value π.

the blank contribution in our data reduction calculations indicates that the Pb–Pb age does not vary with blank contribution. Rather, the error increases with increasing blank contribution.

Other mechanisms that could disturb the U–Pb systematics of 78238 and produce the spread in observed ages are: (1) a change in the $^{238}\text{U}/^{235}\text{U}$ ratio due to neutron capture (Reedy, 1981), (2) impact volatilization and deposition of volatilized lunar Pb, (3) loss of U-series intermediate daughter products (Frisen and Heymann, 1972; Unruh and Tatsumoto, 1977), and (4) preferential loss of Pb relative to U during laboratory handling (e.g., Premo and Tatsumoto, 1992). Neutron capture occurring on the lunar surface has been postulated to change the $^{238}\text{U}/^{235}\text{U}$ ratio from its nominal value of 137.88 (Reedy, 1981). However, the $^{238}\text{U}/^{235}\text{U}$ ratio of 78238 must be lowered to 84.10 in order for the two U–Pb ages to be concordant. Such an extreme deviation from the nominal value, coupled with the measurements of $^{238}\text{U}/^{235}\text{U}$ in lunar materials by Chen and Wasserburg (1981) that indicates no notable deviation from 137.88, does not support a change in the $^{238}\text{U}/^{235}\text{U}$ ratio as the mechanism that caused the difference in U–Pb ages for 78238. Impact volatilization of Pb will increase the μ values of the fractions if Pb is lost, generating a spread in ages with Pb–Pb > ^{235}U–^{207}Pb > ^{238}U–^{206}Pb. However, this mechanism decreases all three of the ages relative to the Sm–Nd crystallization age, and is unlikely to be responsible for the disturbed U–Pb systematics in 78238 because the Pb–Pb age is concordant with the Sm–Nd crystallization age. Loss of U-series daughter products, specifically isotopes of Rn gas, can explain the difference in the two U–Pb ages. The longer-lived ^{222}Rn (part of the ^{238}U decay chain, $t_{1/2} = 3.82$ days) may escape more readily from the system than its counterpart on the ^{235}U decay chain (^{219}Rn, $t_{1/2} = 3.96$ s). However, to explain the difference between the crystallization age and the ^{238}U–^{206}Pb age, preferential diffusion of ^{222}Rn must have occurred over an unreasonably long period (~800 Ma).

Preferential loss of Pb over U during sample handling (e.g., crushing, mineral separating, or leaching) could cause the differences in ages without changing the Pb isotopic composition of the mineral fractions (e.g., Premo and Tatsumoto, 1992). Leachates of 78238 mineral fractions were not analyzed during this study because they are assumed to be mixtures of terrestrial contamination from sample handling, adsorbed lunar surface Pb, and sample Pb (e.g., Premo and Tatsumoto, 1991). However, a 25–28% preferential removal of (lunar) Pb from the mineral fractions could account for the discrepancies in ages between the U–Pb isotopic system and the Sm–Nd, Rb–Sr, and Pb–Pb isotopic systems. Importantly, this process will not influence the Pb–Pb age because Pb isotopes are not fractionated. Thus, it is likely that U–Pb fractionation during sample handling is the disturbance mechanism. It is interesting to note that apparent fractionation of U and Pb during leaching are observed in the most highly shocked lunar and martian samples (e.g., Premo and Tatsumoto, 1992; Misawa et al., 1997). This suggests that leaching-induced fractionation is facilitated by the shock process.

The μ value for the 78238 source is calculated using a time-averaged, single-stage growth model (4558–4334 Ma) on Fig. 7b, and the mineral fractions that do not appear to be disturbed. The data intersect a single-stage growth curve with a μ value of 27 ± 30 at 4334 Ma. The relatively large error associated with the μ value of the 78238 source is the result of the length the 78238 data must be projected to intersect the growth curve. A similar projection on the $^{206}\text{Pb}/^{204}\text{Pb}$ vs. $^{207}\text{Pb}/^{204}\text{Pb}$ diagram yields results that are consistent, but suffers due to both the length of the projection to the growth curve and the large uncertainty on both axes of the diagram. As a result, we prefer the calculation based on the $^{204}\text{Pb}/^{206}\text{Pb}$ and $^{207}\text{Pb}/^{206}\text{Pb}$ ratios in Fig. 7b.

Although the source μ value estimated for 78238 is significantly lower than the μ estimated for the single-stage growth of the source of 78235 and 78236 (μ ~508) by Premo and Tatsumoto (1991), it is close to the source μ for
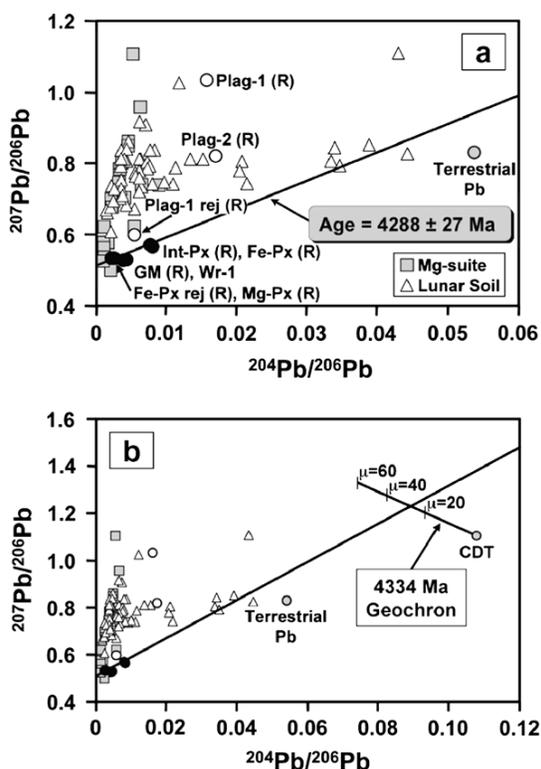
Fig. 7. (a) $^{204}Pb/^{206}Pb$ vs. $^{207}Pb/^{206}Pb$ diagram illustrating the similarity between the Pb isotopic composition of the 78238 plagioclase fractions and lunar soil (Premo et al., 1999). The age for 78238 determined from this Pb representation is 4288 ± 27 Ma (MSWD = 6925), and excludes the plagioclase fractions. Note the relatively low $^{207}Pb/^{206}Pb$ ratio of 78238 when compared to other Mg-suite whole rocks (Premo et al., 1999). (b) Expanded version of (a) with an extension of the linear regression. The line intersects the 4334 Ma geochron at $^{204}Pb/^{206}Pb$ and $^{207}Pb/^{206}Pb$ ratios equivalent to single-stage growth from Canyon Diablo Troilite (CDT) in a reservoir with a μ ($^{238}U/^{204}Pb$) value of 27 ± 30.

mare basalt Yamato-793168 (22 ± 4; Torigoye-Kita et al., 1995) and within error of the source μ of mare basalt Asuka-881757 (10 ± 3; Misawa et al., 1993). It is also within error of the μ value calculated for the time-integrated source region for mare basalt 10017 (70 ± 30; Gaffney et al., 2007), and very close to the μ value calculated for 60025 (~35) by Premo and Tatsumoto (1992). The relatively low μ value calculated for 78238 contradicts the excessively high μ values for the bulk Moon calculated in previous studies.

High estimates for the μ value of the bulk Moon stem from the high source μ values calculated for KREEP-rich rocks. These estimates tend to be made using the intersection of a best-fit line and a concordia diagram (e.g., Premo and Tatsumoto, 1991). However, the concordia diagram is susceptible to disturbance associated with U and Pb fractionation during sample handling. Disturbance of the U–Pb isotopic systematics by the lunar cataclysm may also result in discordia that intercept the concordia line at shallow angles and therefore result in large uncertainties. We therefore feel that source μ values are most accurately estimated

from either Pb–Pb or U–Pb isochron plots that yield ages concordant with crystallization ages determined by other means.

High μ values for KREEP are expected because KREEP is thought to be the latest-stage, most incompatible element-enriched material on the Moon. Any fractionation of U from Pb during LMO solidification by silicates or sulfides is expected to increase the μ value of KREEP (e.g., Neal and Ely, 2002; Gaffney et al., 2007). Therefore, KREEP-rich samples potentially define the maximum bulk Moon μ value. Thus, the μ value estimated for 78238 can be used to constrain the bulk Moon μ value. For example, if there was no fractionation of U and Pb during differentiation of the Moon, then 27 ± 30 is a reasonable estimate for the bulk lunar μ value. If silicates fractionated U from Pb during the formation of KREEP, with U being slightly more incompatible than Pb, then the bulk lunar μ value is less than the maximum 78238 source μ value of 57. If sulfides formed before KREEP during LMO solidification (e.g., Neal and Ely, 2002), removing the majority of Pb from the system and significantly increasing the μ value of KREEP, then the bulk lunar μ value is likely to be significantly less than 57. Regardless of the amount of fractionation of U and Pb that occurred during LMO solidification, the bulk lunar μ value is probably less than 57. Thus, lunar μ values are similar to those estimated for the Earth (<10; e.g., Stacey and Kramers, 1975) and Mars (~2–5; Chen and Wasserburg, 1986; Borg et al., 2005a; Gaffney et al., 2006).

5. IMPLICATIONS AND CONCLUSIONS

The Sm–Nd isochron for 78238 defines an age of 4334 ± 37 Ma with an initial ε_{Nd}^{143} value of -0.27 ± 0.74. The Sm–Nd isotopic systematics of 78238 are consistent with the modeled crystallization sequence of the LMO, and indicates that the Mg-suite is younger than the time of KREEP formation. Sample 78238 therefore places a minimum constraint on the time of LMO solidification. Additional constraints can be placed on the formation age of KREEP by considering the time and initial ε_{Nd}^{143} values of Mg-suite and KREEP basalts. Applying these constraints yields a calculated differentiation age of KREEP of 4492 ± 61 Ma. This model age indicates a relatively early differentiation of a CHUR-like bulk Moon. It further suggests that Mg-suite magmatism started later than previously thought.

The two ages obtained by the Rb–Sr isotopic system for 78238 are 4366 ± 53 Ma (C) and 4003 ± 95 Ma (M). The (C) isochron is concordant with the Sm–Nd age for 78238, and is indicative of crystallization. The (M) isochron is concordant with an Ar–Ar age on a plagioclase separate from 78236. The two different isochrons may be a result of isotopic re-equilibration of interstitial material in the majority of the mineral fractions during a shock metamorphism event.

Multiple "ages" were obtained for 78238 during analysis of the U–Pb isotopic systematics. The Pb–Pb isochron indicated a crystallization age for 78238 of 4333 ± 59 Ma and is concordant with both the Sm–Nd and Rb–Sr (C) ages.

Unfortunately, the U–Pb isotopic systems appear to be disturbed. The ^{235}U–^{207}Pb linear array indicates an age for 78238 of 4010 ± 60 Ma, and the ^{238}U–^{206}Pb "age" is 3520 ± 290 Ma. We hypothesize that fractionation of U and Pb occurred during sample handling and/or leaching of the mineral fractions because other potential disturbances fail to account for all of the observed U–Pb isotopic systematics. A single-stage source μ value of 27 ± 30 was calculated for 78238 and is consistent with a bulk lunar μ value similar to the Earth and Mars.

ACKNOWLEDGMENTS

REFERENCES

Aeschlimann U., Eberhardt P., Geiss J., Grögler N., Kurtz J. and Marti K. (1982) On the age of cumulate norite 78236: an ^{39}Ar–^{40}Ar study. *Lunar Planet. Sci. XIII*. Lunar Planet. Inst., Houston. #1–2 (abstr.).

Alibert C. (1994) Erratum to Alibert, C., Norman, M.D., McCulloch, M.T. (1994) An ancient Sm–Nd age for a ferroan noritic anorthosite clast from lunar breccia 67016. *Geochim. Cosmochim. Acta* **58**, 5369.

Alibert C., Norman M. D. and McCulloch M. T. (1994) An ancient Sm–Nd age for a ferroan noritic anorthosite clast from lunar breccia 67016. *Geochim. Cosmochim. Acta* **58**, 2921–2926.

Amelin Y. and Rotenberg E. (2004) Sm–Nd systematics of chondrites. *Lunar Planet. Sci. XXXV*. Lunar Planet. Inst., Houston. #1322 (abstr.).

Arndt J. and Gonzalez-Cabeza I. (1981) Diaplectic glass and fusion-formed glass: comparative studies on shocked anorthosite from Manicouagan Crater, Canada. *Lunar Planet. Sci. XII*. Lunar Planet. Inst., Houston. #28–30 (abstr.).

Borg L. E., Nyquist L. E., Taylor L. A., Wiesmann H. and Shih C.-Y. (1997) Constraints on martian differentiation processes from Rb–Sr and Sm–Nd isotopic analyses of the basaltic shergottite QUE 94201. *Geochim. Cosmochim. Acta* **61**, 4915–4931.

Borg L. E. and Draper D. S. (2003) A petrogenetic model for the origin and compositional variation of the martian basaltic meteorites. *Meteor. Planet. Sci.* **38**, 1713–1731.

Borg L. E. and Drake M. J. (2005) A review of meteorite evidence for the timing of magmatism and of surface or near-surface liquid water on mars. *J. Geophys. Res.* **110**, E12S03. doi:10.1029/2005JE002402.

Borg L. E. and Wadhwa M. (2006) ε^{142}Nd–ε^{143}Nd isotopic evidence for protracted lunar differentiation. *Lunar Planet. Sci. XXXVII*. Lunar Planet. Inst., Houston. #1154 (abstr.).

Borg L., Norman M., Nyquist L., Bogard D., Snyder G., Taylor L. and Lindstrom M. (1999) Isotopic studies of ferroan anorthosite 62236: a young lunar crustal rock from a light rare-earth-element-depleted source. *Geochim. Cosmochim. Acta* **63**, 2679–2691.

Borg L. E., Shearer C. K., Asmerom Y. and Papike J. J. (2004) Prolonged KREEP magmatism on the Moon indicated by the youngest dated lunar igneous rock. *Nature* **432**, 209–211.

Borg L. E., Edmunson J. E. and Asmerom Y. (2005a) Constraints on the U–Pb isotopic systematics of Mars inferred from a combined U–Pb, Rb–Sr, and Sm–Nd isotopic study of the martian meteorite Zagami. *Geochim. Cosmochim. Acta* **69**, 5819–5830.

Borg L. E., Shearer C. K., Asmerom Y. and Papike J. J. (2005b) Geochemical and isotopic systematics of the youngest dated lunar igneous rock, Northwest Africa 773. *Lunar Planet. Sci. XXXVI*. Lunar Planet. Inst., Houston. #1026 (abstr.).

Boyet M. and Carlson R. W. (2005) ^{142}Nd evidence for early (>4.53 Ga) global differentiation of the silicate Earth. *Science* **309**, 576–581.

Carlson R. W. and Lugmair G. W. (1979) Sm–Nd constraints on early lunar differentiation and the evolution of KREEP. *Earth Planet. Sci. Lett.* **45**, 123–132.

Carlson R. W. and Lugmair G. W. (1981) Time and duration of lunar highlands crust formation. *Earth Planet. Sci. Lett.* **52**, 227–238.

Carlson R. W. and Lugmair G. W. (1988) The age of ferroan anorthosite 60025: oldest crust on a young Moon? *Earth Planet. Sci. Lett.* **90**, 119–130.

Caro G., Bourdon B., Halliday A. N. and Quitté G. (2008) Super-chondritic Sm/Nd ratios in Mars, the Earth and the Moon. *Nature* **452**, 336–339.

Chen J. H. and Wasserburg G. J. (1981) Isotopic determination of uranium in picomole and subpicomole quantities. *Anal. Chem.* **53**, 2060–2067.

Chen J. H. and Wasserburg G. J. (1986) Formation ages and evolution of Shergotty and its parent planet from U–Th–Pb systematics. *Geochim. Cosmochim. Acta* **50**, 955–968.

Duke M. B. (1968) The Shergotty meteorite: magmatic and shock metamorphism features. In *Shock Metamorphism of Natural Materials* (eds. N. M. Short and B. M. French). Mono Book Corp., Baltimore, pp. 613–621.

El Goresy A., Engelhardt W. V., Arndt J. and Manglier D. (1976) Shocked norite 78235: primary textures and shock features. *Lunar Sci. VII*. Lunar Planet. Inst., Houston. #239–241 (abstr.).

Fletcher I. R. and Rosman K. J. R. (1982) Precise determination of initial ε_{Nd} from Sm–Nd isochron data. *Geochim. Cosmochim. Acta* **46**, 1983–1987.

Foley C. N., Wadhwa M., Borg L. E., Janney P. E., Hines R. and Grove T. L. (2005) The early differentiation history of Mars from ^{182}W–^{142}Nd isotope systematics in the SNC meteorites. *Geochim. Cosmochim. Acta* **69**, 4557–4571.

Frisen L. J. and Heymann D. (1972) Model for radon diffusion through the lunar regolith. *Moon* **3**, 461–471.

Gaffney A. M., Borg L. E. and Connelly J. N. (2006) U–Pb isotope systematics of shergottite Queen Alexandra Range 94201: seeing through terrestrial lead contamination to identify an even lower-mu source on Mars. *Lunar Planet. Sci.*. Lunar Planet. Inst., Houston. #1483 (abstr.).

Gaffney A. M., Borg L. E. and Asmerom Y. (2007) U–Pb systematics in mare basalt source regions: a combined U–Pb, Rb–Sr. and Sm–Nd study of mare basalt 10017. *Geochim. Cosmochim. Acta* **71**, 3656–3671.

Hanan B. B. and Tilton G. R. (1987) 60025: Relict of primitive lunar crust? *Earth Planet. Sci. Lett.* **84**, 15–21.

Hinthorne J. R., Conrad R. L. and Church S. E. (1977) Lead–lead age and rare earth element determinations in lunar norite 78235. *Lunar Planet. Sci. VIII*. Lunar Planet. Inst., Houston. #444–446 (abstr.).

Jackson E. D., Sutton R. L. and Wilshire H. G. (1975) Structure and petrology of a cumulus norite boulder sampled by Apollo 17 in Taurus-Littrow Valley, the Moon. *Geol. Soc. Am. Bull.* **86**, 433–442.

James O.B. and Flohr M. K. (1983) Subdivision of the Mg-suite noritic rocks into Mg-gabbronorites and Mg-norites. *Proceedings of the 13th Lunar Planet. Sci., J. Geophys. Res.* **88**, A603–A614.

Korotev R. L., Haskin L. A. and Lindstrom M. M. (1980) A synthesis of lunar highlands compositional data. *Proceedings of the 11th Lunar Planet. Sci.* Lunar Planet. Inst., Houston. 395–429.

Ludwig K. R. (2001) Isoplot/Ex rev. 2.49; a geochronological toolkit for Microsoft Excel. *Berkeley Geochronology Center Special Publication No. 1a*.

Lugmair G. W. and Carlson R. W. (1978) The Sm–Nd history of KREEP. *Proceedings of the Ninth Lunar Planet. Sci.* Lunar Planet. Inst., Houston. 689–704.

Lugmair G. W., Marti K., Kurtz J. P. and Scheinin N. B. (1976) History and genesis of lunar troctolite 76535. *Proceedings of the Seventh Lunar Sci.* Lunar Planet. Inst., Houston. 2009–2033.

McCallum I. S. and Mathez E. A. (1975) Petrology of noritic cumulates and a partial melting model for the genesis of Fra Mauro basalts. *Proceedings of the Sixth Lunar Sci.* Lunar Planet. Sci., Houston. 395–414.

Mehta S. and Goldstein J. I. (1980) Metallic particles in the glassy constituents of three lunar highland samples 65316, 67435 and 78235. *Proceedings of the 11th Lunar Planet. Sci.* Lunar Planet. Inst., Houston. 1713–1725.

Minster J.-F., Birck J.-L. and Allègre C. J. (1982) Absolute age of formation of chondrites studied by the ^{87}Rb–^{87}Sr method. *Nature* **300**, 414–419.

Misawa K., Tatsumoto M., Dalrymple G. B. and Yanai K. (1993) An extremely low U/Pb source in the Moon: U–Th–Pb, Sm–Nd, Rb–Sr, and Ar/Ar isotopic systematics and age of lunar meteorite Asuka-881757. *Geochim. Cosmochim. Acta* **57**, 4687–4702.

Misawa K., Nakamura N., Premo W. R. and Tatsumoto M. (1997) U–Th–Pb isotopic systematics of lherzolitic shergottite Yama-to-793605. *Ant. Meteor. Res.* **10**, 95–108.

Misawa K., Yamazaki F., Sawads S., Sekine T. and Nakamura N. (2000) Incorporation of radiogenic lead into plagioclase during shock metamorphism. *Meteor. Planet. Sci.* **35**(Suppl.), A111 (abstr.).

Nägler Th. F. and Kramers J. D. (1998) Nd isotopic evolution of the upper mantle during the Precambrian: models, data and the uncertainty of both. *Precamb. Res.* **91**, 233–252.

Nakamura N., Tatsumoto M., Nunes P. D., Unruh D. M., Schwab A. P. and Wildeman T. R. (1976) 4.4 b.y.-old clast in Boulder 7, Apollo 17: a comprehensive chronological study by U–Pb, Rb–Sr and Sm–Nd methods. *Proceedings of the Seventh Lunar Sci.* Lunar Planet. Inst., Houston. 2309–2333.

Neal C. R. and Ely J. C. (2002) Sulfide immiscibility in the lunar magma ocean: evidence for a primitive lunar lower mantle and the origin of high-μ mare basalts. *Lunar Planet. Sci. XXXIII.* Lunar Planet. Inst., Houston. #1821 (abstr.).

Nemchin A. A., Pidgeon R. T., Whitehouse M. J., Vaughan J. P. and Meyer C. (2008) SIMS U–Pb study of zircon from Apollo 14 and 17 breccias: implications for the evolution of lunar KREEP. *Geochim. Cosmochim. Acta* **72**, 668–689.

Norman M. D., Borg L. E., Nyquist L. E. and Bogard D. D. (2003) Chronology, geochemistry, and petrology of a ferroan noritic anorthosite clast from Descartes breccia 67215: clues to the age, origin, structure, and impact history of the lunar crust. *Meteor. Planet. Sci.* **38**, 645–661.

Nyquist L. E. (1977) Lunar Rb–Sr chronology. *Phys. Chem. Earth* **10**, 103–142.

Nyquist L. E. and C.-Y. Shi (1992) The isotopic record of lunar volcanism. *Geochim. Cosmochim. Acta* **56**, 2213–2234.

Nyquist L. E., Hubbard N. J., Gast P. W., Church S. E., Bansal B. M. and Wiesmann H. (1972) Rb–Sr systematics for chemically defined Apollo 14 breccias. *Proceedings of the Third Lunar Sci.* Lunar Planet. Inst., Houston. 1515–1530.

Nyquist L. E., Hubbard N. J., Gast P. W., Bansal B. M., Wiesmann H. and Jahn B.-M. (1973) Rb–Sr systematics for chemically defined Apollo 15 and 16 materials. *Proceedings of the Fourth Lunar Sci.* Lunar Planet. Inst., Houston. 1823–1846.

Nyquist L. E., Bansal B. M., Wiesmann H. and Jahn B.-M. (1974) Taurus-Littrow chronology: some constraints on early lunar crustal development. *Proceedings of the Fifth Lunar Sci.* Lunar Planet. Inst., 1515–1539.

Nyquist L. E., Reimold W. U., Bogard D. D., Wooden J. L., Bansal B. M., Wiesmann H. and Shih C.-Y. (1981) A comparative Rb–Sr, Sm–Nd, and K–Ar study of shocked norite 78236: evidence of slow cooling in the lunar crust? *Proceedings of the 12th Lunar Planet. Sci.* Lunar Planet. Inst., Houston. 67–97.

Nyquist L. E., Bogard D. D., Garrison D. H., Bansal B. M., Wiesmann H. and Shih C.-Y. (1991a) Thermal resetting of radiometric ages. I: Experimental investigation. *Lunar Planet. Sci. XXII.* Lunar Planet Inst., Houston. #985–986 (abstr.).

Nyquist L. E., Bogard D. D., Garrison D. H., Bansal B. M., Wiesmann H. and Shih C.-Y. (1991b) Thermal resetting of radiometric ages. II: Modeling and applications. *Lunar Planet. Sci. XXII.* Lunar Planet Inst., Houston. #987–988 (abstr.).

Nyquist L. E., Bansal B., Wiesmann H. and Shih C.-Y. (1994) Neodymium, strontium and chromium isotopic studies of the LEW 86010 and Angra dos Reis meteorites and the chronology of the angrite parent body. *Meteorites* **29**, 872–885.

Nyquist L. E., Wiesmann H., Bansal B., Shih C.-Y., Keith J. E. and Harper C. L. (1995) ^{146}Sm–^{142}Nd formation interval for the lunar mantle. *Geochim. Cosmochim. Acta* **59**, 2817–2837.

Nyquist L. E., Shih C.-Y. and Takeda H. (2004) Chronology of eucrite petrogenesis from Sm–Nd and Rb–Sr systematics. Antarctic Meteorites XXVIII. National Inst. of Polar Res., Tokyo. 66–67 (abstr.).

Nyquist L., Bogard D., Yamaguchi A., Shih C.-Y., Karouji Y., Ebihara M., Reese Y., Garrison D., McKay G. and Takeda H. (2006) Feldspathic clasts in Yamato 86032: remnants of the lunar crust with implications for its formation and impact history. *Geochim. Cosmochim. Acta* **70**, 5990–6015.

Nyquist L. E., Shih C.-Y. and Reese Y. D. (2008) Sm–Nd for norite 78236 and eucrite Y980318/433: implications for planetary and solar system processes. *Lunar Planet. Sci. XXXIX.* Lunar Planet. Inst., Houston. #1437 (abstr.).

Palme H. (1977) On the age of KREEP. *Geochim. Cosmochim. Acta* **41**, 1791–1801.

Papanastassiou D. A. and Wasserburg G. J. (1969) Initial strontium isotopic abundances and the resolution of small time differences in the formation of planetary objects. *Earth Planet. Sci. Lett.* **5**, 361–376.

Papanastassiou D. A. and Wasserburg G. J. (1975) Rb–Sr study of a lunar dunite and evidence for early lunar differentiates. *Proceedings of the Sixth Lunar Sci.* Lunar Planet. Inst., Houston. 1467–1489.

Papanastassiou D. A. and Wasserburg G. J. (1976) Rb–Sr age of troctolite 76535. *Proceedings of the Seventh Lunar Sci.* Lunar Planet. Inst., Houston. 2035–2054.

Papike J. J., Simon S. B. and Laul J. C. (1982) The lunar regolith: chemistry, mineralogy, and petrology. *Rev. Geophys. Space Phys.* **20**, 761–826.

Papike J. J., Fowler G. W., Shearer C. K. and Layne G. D. (1996) Ion microprobe investigation of plagioclase and orthopyroxene from lunar Mg-suite norites: implications for calculating parental melt REE concentrations and for assessing postcrys-

tallization REE redistribution. *Geochim. Cosmochim. Acta* **60**, 3967–3978.

Premo W. R. (1991) Rb–Sr and Sm–Nd ages for lunar norite 78235/78236: implications on the U–Pb isotopic systematics of this high-Mg rock. *Lunar Planet. Sci. XXII*. Lunar Planet. Inst., Houston. #1089–1090 (abstr.).

Premo W. R. and Tatsumoto M. (1991) U–Th–Pb isotopic systematics of lunar norite 78235. *Proceedings of the 21st Lunar Planet. Sci.* Lunar Planet. Inst., Houston. 89–100.

Premo W. R. and Tatsumoto M. (1992) U–Th–Pb, Rb–Sr, and Sm–Nd isotopic systematics of lunar troctolitic cumulate 76535: implications on the age and origin of this early lunar, deep-seated cumulate. *Proceedings of the 22nd Lunar Planet. Sci.* Lunar Planet. Inst., Houston. 381–397.

Premo W. R., Tatsumoto M., Misawa K., Nakamura N. and Kita N. I. (1999) Pb-isotopic systematics of lunar highland rocks (>3.9 Ga): constraints on early lunar evolution. In *Planetary Petrology and Geochemistry* (eds. G. A. Snyder, C. R. Neal and W. G. Ernst), vol. 2, pp. 207–240.

Rankenburg K., Brandon A. D. and Neal C. R. (2006) Neodymium isotope evidence for a chondritic composition of the Moon. *Science* **312**, 1369–1372.

Reedy R. C. (1981) Cosmic-ray produced stable nuclides: various production rates and their implications. *Proceedings of the 12th Lunar Planet. Sci.* Lunar Planet. Inst., Houston. 1809–1823.

Sclar C. B. and Bauer J. F. (1975) Shock-induced subsolidus reduction-decomposition of orthopyroxene and shock-induced melting in norite 78235. *Proceedings of the Sixth Lunar Sci.* Lunar Planet. Inst., Houston. 799–820.

Shearer C. K. and Papike J. J. (1999) Magmatic evolution of the Moon. *Am. Min.* **84**, 1469–1494.

Shih C.-Y., Nyquist L. E., Bogard D. D., Wooden J. L., Bansal B. M. and Wiesmann H. (1985) Chronology and petrogenesis of a 1.8g lunar granite clast: 14321,1062. *Geochim. Cosmochim. Acta* **49**, 411–426.

Shih C.-Y., Nyquist L. E., Bansal B. M. and Wiesmann H. (1992) Rb–Sr and Sm–Nd chronology of an Apollo 17 KREEP basalt. *Earth Planet. Sci. Lett.* **108**, 203–215.

Shih C.-Y., Nyquist L. E., Dasch E. J., Bogard D. D., Bansal B. M. and Wiesmann H. (1993) Ages of pristine noritic clasts from lunar breccias 15445 and 15455. *Geochim. Cosmochim. Acta* **57**, 915–931.

Smith J. V., Anderson A. T., Newton R. C., Olsen E. J., Wyllie P. J., Crewe A. V., Isaacson M. S. and Johnson D. (1970) Petrologic history of the moon inferred from petrography, mineralogy, and petrogenesis of Apollo 11 rocks. *Proceedings of the Apollo 11 Sci.* Lunar Planet. Inst., Houston. 897–925.

Snyder G. A., Taylor L. A. and Neal C. R. (1992) A chemical model for generating the sources of mare basalts: combined equilibrium and fractional crystallization of the lunar magma-sphere. *Geochim. Cosmochim. Acta* **56**, 3809–3823.

Snyder G. A., Taylor L. A. and Halliday A. N. (1995) Chronology and petrogenesis of the lunar highlands alkali suite: cumulates from KREEP basalt crystallization. *Geochim. Cosmochim. Acta* **59**, 1185–1203.

Stacey J. S. and Kramers J. D. (1975) Approximation of terrestrial lead isotope evolution by a two-stage model. *Earth Planet. Sci. Lett.* **26**, 207–221.

Taylor D. J., McKeegan K. D., Harrison T. M. and McCulloch M. (2007) ^{176}Lu–^{176}Hf in lunar zircons: identification of an early enriched reservoir on the Moon. *Lunar and Planetary Science XXXVIII*, #2130 (abstr.).

Tera F. and Wasserburg G. J. (1972) U–Th–Pb systematics in lunar highland samples from the Luna 20 and Apollo 16 missions. *Earth Planet. Sci. Lett.* **17**, 36–51.

Torigoye-Kita N., Misawa K., Dalrymple G. B. and Tatsumoto M. (1995) Further evidence for a low U/Pb source in the Moon: U–Th–Pb, Sm–Nd, and Ar–Ar isotopic systematics of lunar meteorite Yamato-793169. *Geochim. Cosmochim. Acta* **59**, 2621–2632.

Unruh D. M. and Tatsumoto M. (1977) Evolution of mare basalts: the complexity of the U–Th–Pb system. *Proceedings of the Eighth Lunar Planet. Sci.* Lunar Planet. Inst., Houston. 1673–1696.

Winzer S. R., Lum R. K. L., Schuhmann S. and Philpotts J. A. (1975) Large ion lithophile trace element abundances in phases from 78235, 34, a lunar norite cumulate. *Lunar Sci. VI*. Lunar Planet. Inst., Houston. #872–874 (abstr.).

Wood J. A., Dickey J. S., Marvin U. B. and Powell B. N. (1970) Lunar anorthosites and a geophysical model of the Moon. *Proceedings of the Apollo 11 Sci.* Lunar Planet. Inst., Houston. 965–988.

Associate editor: Noriko T. Kita